Journal of Coordination Chemistry

ISSN: 0095-8972 (Print) 1029-0389 (Online) Journal homepage: http://www.tandfonline.com/loi/gcoo20

Syntheses, crystal structures and antibacterial activities of M(II) benzene-1,2,3-triyltris(oxy)triacetic acid complexes

Hui-Liang Wen, Bo-Wen Lai, Hai-Wei Hu & Yun-Han Wen

To cite this article: Hui-Liang Wen, Bo-Wen Lai, Hai-Wei Hu & Yun-Han Wen (2015) Syntheses, crystal structures and antibacterial activities of M(II) benzene-1,2,3-triyltris(oxy)triacetic acid complexes, Journal of Coordination Chemistry, 68:21, 3903-3917, DOI: 10.1080/00958972.2015.1082554

To link to this article: http://dx.doi.org/10.1080/00958972.2015.1082554

Accepted author version posted online: 14 Aug 2015.
Published online: 14 Sep 2015.

Journal of Coordination Chemistry, 2015
Vol. 68, No. 21, 3903–3917, http://dx.doi.org/10.1080/00958972.2015.1082554

Syntheses, crystal structures and antibacterial activities of M(II) benzene-1,2,3-triyltris(oxy)triacetic acid complexes

HUI-LIANG WEN*†, BO-WEN LAI‡, HAI-WEI HU† and YUN-HAN WEN§

†State Key Laboratory of Food Science and Technology, Nanchang University, Nanchang, PR China
‡Chemicals Analysis Department, Nanchang Institute for Food and Drug Control, Nanchang, PR China
§School of Chemistry and Biochemistry, The Ohio State University-Columbus, Columbus, OH, USA

(*Received 5 February 2015; accepted 27 July 2015*)

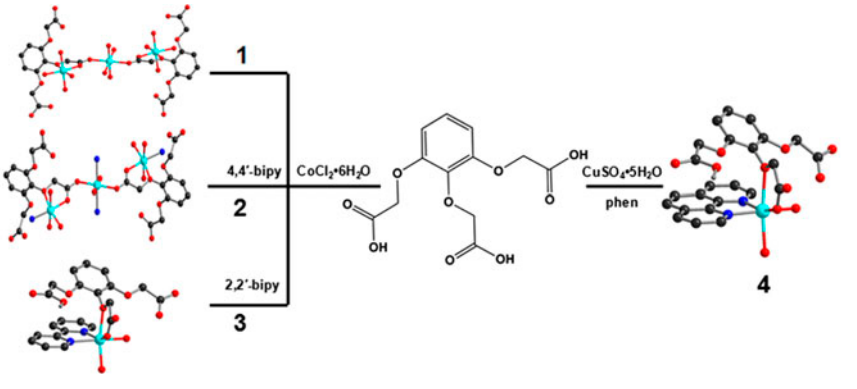

Four metal(II) complexes with benzene-1,2,3-triyltris(oxy)triacetic acid (H_3L), $\{[Co_{1.5}(L)(H_2O)_6]\cdot 6H_2O\}_n$ (**1**), $\{[Co_{1.5}(L)(4,4'\text{-bipy})_{1.5}(H_2O)_4]\cdot 4H_2O\}_n$ (**2**), $\{[Co(HL)(2,2'\text{-bipy})(H_2O)_2]\cdot 1.5H_2O\}_n$ (**3**), and $\{[Cu(HL)(phen)(H_2O)_2]\cdot H_2O\}_n$ (**4**) (4,4′-bipy = 4,4′-bipyridine; 2,2′-bipy = 2,2′-bipyridine; phen = phenanthroline), were prepared and structurally characterized. Complex **2** displays a 1-D structure, while **1**, **3**, and **4** reveal 0-D structures, which further extend to 3-D supramolecular networks by hydrogen bonding interactions, of which **1** and **4** contain double-helical chains, **2** includes meso-helices, and **3** comprises single-helices. Furthermore, the thermal stabilities and antibacterial activities of the complexes were studied.

Keywords: Benzene-1,2,3-triyltris(oxy)triacetic acid; Transition metal complexes; N-Donor co-ligands; Helix; Antibacterial activity

1. Introduction

Self-assembly of supramolecular architectures by the process of non-covalent interactions including coordination bonding, hydrogen bonding, and $\pi\cdots\pi$ stacking interactions has

*Corresponding author. Email: hlwen70@163.com

been a very active area of crystal engineering [1–10]. Supramolecular assembly is a central theme in the design of classes of crystalline materials with intriguing topologies and structural diversities, such as helical, herringbone, honeycomb, and other geometries [11–14], and potential functions in magnetic behavior, optical materials, and biological activities [15–17]. Polycarboxylic acids are frequently utilized to construct supramolecular architectures and our group has constructed some intriguing architectures utilizing polycarboxylate ligands [18–33]. Polycarboxylic acids exhibit diverse coordination modes and are good candidates for hydrogen-bond acceptors and donors, so that they can act as effective building blocks for high-dimensional supramolecular structures. In our continuing work, we synthesized a new polycarboxylate ligand, benzene-1,2,3-triyltris(oxy)triacetic acid (H_3L), which possesses several interesting characteristics: (a) it has three $–OCH_2COOH$ groups which may be partially or completely deprotonated to generate H_2L^-, HL^{2-}, or L^{3-} according to different reaction conditions; (b) three $–OCH_2COOH$ groups branch out at angles of 60° and 120°, which can furnish various coordination modes and allow structure diversities; and (c) it can serve not only as a hydrogen-bond acceptor, but also as a hydrogen-bond donor, depending upon the numbers of deprotonated carboxylate groups and whether the groups are interacting with the metal ions or not. All of these features help H_3L to construct helical structures with metal ions.

Owing to its $–OCH_2COOH$ groups, phenoxy acetic acid compounds exhibit superior antibacterial activities. For example, Pan reported that 2-(4-((3-(4-methoxybenzyl)-2-(4- methoxybenzylimino)-4-oxothiazolidin-5-ylidene)methyl)phenoxy)acetic acid displayed good activity against *Staphylococcus epidermidis* [34] and Zhao reported that 2-(4-((6-(ethoxycarbonyl)-3-oxo-5-phenyl-3,5-dihydro-2H-thiazolo[3,2-a]pyrimidin-2-ylidene) methyl)phenoxy)acetic acid derivatives showed favorable activity against *S. epidermidis* and *Staphylococcus aureus* [35].

N-donor co-ligands, such as 4,4′-bipy, 2,2′-bipy and phen, are appropriate auxiliary ligands for constructing supramolecular structures via hydrogen bonds and/or $\pi\cdots\pi$ stacking interactions [36–38]. Herein, we report the structures and the antibacterial activities of four transition metal complexes with benzene-1,2,3-triyltris(oxy)triacetic acid with or without N-donor co-ligands: $\{[Co_{1.5}(L)(H_2O)_6]\cdot 6H_2O\}_n$ (**1**), $\{[Co_{1.5}(L)(4,4'\text{-bipy})_{1.5}(H_2O)_4]\cdot 4H_2O\}_n$ (**2**), $\{[Co(HL)(2,2'\text{-bipy})(H_2O)_2]\cdot 1.5H_2O\}_n$ (**3**), and $\{[Cu(HL)(phen)(H_2O)_2]\cdot H_2O\}_n$ (**4**).

2. Experimental

2.1. *Materials and instrumentation*

All reagents were commercially available and used without purification. Elemental analyses of C, H, and N were carried out with a Flash EA 1112 Elemental analyzer. IR spectra were recorded with a Nicolet Avatar 360 FT-IR spectrometer using KBr pellets. Thermogravimetric curves were recorded with a Perkin-Elmer Diamond TG/DTA thermal analyzer; a platinum container was used for heating the sample with a heating rate of 10 °C/min under a N_2 atmosphere.

2.2. *Syntheses of 1–4*

2.2.1. Synthesis of $\{[Co_{1.5}(L)(H_2O)_6]\cdot 6H_2O\}_n$ (1). A mixture of $CoCl_2\cdot 6H_2O$ (0.0238 g, 0.1 mmol), H_3L (0.0300 g, 0.1 mmol), NaOH (0.45 mL, 0.65 mol L^{-1}), and distilled water

(10 mL) was sealed in a new test tube (15 mL) and heated at 90 °C for 5 h under autogenous pressure. Red needle crystals were obtained. Yield: 8.3 mg (20.6% based on Co). Anal. Calcd for $C_{12}H_{33}Co_{1.5}O_{21}$: C, 23.95; H, 5.53%. Found: C, 24.20; H, 5.82%. IR data (KBr pellet, ν/cm^{-1}): 3412 w, 2970 w, 1607 vs 1557 m, 1402 s, 1333 m, 1213 w, 1140 s, 1063 w, 1016 w, 881 w, 768 m, 683 w.

2.2.2. Synthesis of $\{[Co_{1.5}(L)(4,4'\text{-bipy})_{1.5}(H_2O)_4]\cdot 4H_2O\}_n$ (2). A mixture of $CoCl_2\cdot 6H_2O$ (0.0238 g, 0.1 mmol), H_3L (0.0300 g, 0.1 mmol), 4,4′-bipy (0.0156 g, 0.1 mmol), NaOH (0.45 mL, 0.65 mol L^{-1}), and distilled water (10 mL) was sealed in a new test tube (15 mL) and heated at 90 °C for 5 h under autogenous pressure. Red block crystals were obtained. Yield: 12.0 mg (23.5% based on Co). Anal. Calcd for $C_{27}H_{37}Co_{1.5}N_3O_{17}$: C, 42.45; H, 4.88; N, 5.50%. Found: C, 42.76; H, 5.16; N, 5.29%. IR data (KBr pellet, ν/cm^{-1}): 3427 s, 2937 w, 1618 vs 1531 w, 1491 w, 1418 s, 1335 m, 1259 m, 1223 w, 1119 m, 1018 m, 889 w, 822 m, 773 w, 698 m, 642 m, 484 w.

2.2.3. Synthesis of $\{[Co(HL)(2,2'\text{-bipy})(H_2O)_2]\cdot 1.5H_2O\}_n$ (3). The synthesis of **3** was the same as that of **2**, except that 2,2′-bipy was used instead of 4,4′-bipy. Purple-red block crystals were obtained. Yield: 15.2 mg (26.0% based on Co). Anal. Calcd for $C_{22}H_{25}N_2CoO_{12.5}$: C, 45.80; H, 4.34; N, 4.86%. Found: C, 45.25; H, 4.77; N, 4.99%. IR data (KBr pellet, ν/cm^{-1}): 3370 m, 2980 s, 2920 w, 1584 s, 1548 w, 1455 w, 1408 vs 1315 m, 1217 w, 1128 m, 1043 m, 953 w, 841 w, 800 m, 769 m, 689 m.

2.2.4. Synthesis of $\{[Cu(HL)(phen)(H_2O)_2]\cdot H_2O\}_n$ (4). The synthesis of **4** was similar to that of **2**, except that $CuSO_4\cdot 5H_2O$ (0.0250 g, 0.1 mmol) was used instead of 0.1 mmol $CoCl_2\cdot 6H_2O$, and phen (0.0198 g, 0.1 mmol) was used instead of 0.1 mmol 4,4′-bipy. Blue block crystals were obtained. Yield: 17.4 mg (29.2% based on Cu). Anal. Calcd for $C_{24}H_{24}CuN_2O_{12}$: C, 48.37; H, 4.06; N, 4.70%. Found: C, 48.62; H, 4.44; N, 4.33%. IR data (KBr pellet, ν/cm^{-1}): 3533 s, 3329 w, 2924 w, 1693 m, 1608 vs 1522 m, 1418 s, 1339 s, 1256 m, 1122 m, 1018 w, 849 w, 775 w, 725 m, 648 w.

2.3. *X-ray crystallographic study*

The X-ray single-crystal data of **1–4** were recorded on a Bruker APEX II area detector diffractometer with graphite-monochromated Mo-Kα radiation ($\lambda = 0.71073$ Å). Semiempirical absorption corrections were applied to the complexes using SADABS [39]. The structures were solved by direct methods and refined by full-matrix least-squares on F^2 using SHELXL-97 [40]. All non-hydrogen atoms were refined anisotropically. The carboxyl and water hydrogens were located from difference Fourier maps and were included in fixed positions in riding-model approximation with O–H distances of 0.83 Å and with $U_{iso}(H) = 1.5U_{eq}(O)$; the other hydrogens were placed in geometrically calculated positions. Experimental details for X-ray data collection of **1–4** are presented in table 1, selected bond lengths are listed in table 2, and the main hydrogen bonding lengths and angles are listed in table 3.

Table 1. Crystal data for **1–4**.

Complex	1	2	3	4
Empirical formula	$C_{12}H_{33}Co_{1.5}O_{21}$	$C_{27}H_{37}Co_{1.5}N_3O_{17}$	$C_{22}H_{25}CoN_2O_{12.5}$	$C_{24}H_{24}CuN_2O_{12}$
Formula weight	601.78	763.99	576.37	595.99
T [K]	296(2)	296(2)	296(2)	296(2)
Crystal system	Triclinic	Triclinic	Triclinic	Triclinic
Space group	$P\bar{1}$	$P\bar{1}$	$P\bar{1}$	$P\bar{1}$
a (Å)	9.399(2)	10.942(2)	9.729(2)	9.8823(9)
b (Å)	10.132(2)	11.142(2)	11.298(2)	11.690(1)
c (Å)	13.290(3)	15.240(3)	11.939(2)	11.791(1)
α (°)	97.198(3)	109.624(2)	79.366(2)	83.353(1)
β (°)	100.164(3)	103.260(2)	78.421(2)	71.198(1)
γ (°)	97.361(3)	99.150(2)	79.049(2)	81.319(1)
V Å^{-3}	1221.3(5)	1645.9(5)	1247.5(4)	1271.4(2)
Z	2	2	2	2
F(0 0 0)	627	793	596	614
D_c (g cm^{-3})	1.636	1.542	1.534	1.557
θ range (°)	2.39–25.50	2.43–25.50	2.36–25.50	2.38–25.50
μ mm^{-1}	1.123	0.846	0.757	0.928
GOF	1.016	1.016	1.047	1.039
No. data collected	9523	12,716	9701	9890
No. unique data	4518	6080	4618	4696
R_{int}	0.0330	0.0168	0.0204	0.0143
R_1, wR_2 [$I > 2\sigma(I)$]	0.0372, 0.0734	0.0354, 0.0906	0.0423, 0.1112	0.0296, 0.0785
R_1, wR_2 (all data)	0.0594, 0.0817	0.0458, 0.0984	0.0542, 0.1208	0.0333, 0.0808

Table 2. Selected bond lengths (Å) for **1–4**.

1			
Co(1)–O(7)	2.125(2)	Co(1)–O(14)	2.054(2)
Co(1)–O(15)	2.088(2)	Co(2)–O(2)	2.167(2)
Co(2)–O(6)	2.081(2)	Co(2)–O(10)	2.112(2)
Co(2)–O(11)	2.051(2)	Co(2)–O(12)	2.027(2)
Co(2)–O(13)	2.079(2)		
2			
Co(1)–O(6)	2.086(2)	Co(1)–O(13)	2.082(2)
Co(1)–N(1)	2.185(2)	Co(2)–O(2)	2.178(2)
Co(2)–O(7)	2.048(2)	Co(2)–O(10)	2.087(2)
Co(2)–O(11)	2.155(2)	Co(2)–O(12)	2.059(2)
Co(2)–N(3)	2.116(2)		
3			
Co(1)–O(2)	2.232(2)	Co(1)–O(7)	2.014(2)
Co(1)–O(10)	2.060(2)	Co(1)–O(11)	2.086(2)
Co(1)–N(1)	2.116(3)	Co(1)–N(2)	2.131(2)
4			
Cu(1)–O(2)	2.339(1)	Cu(1)–O(6)	1.972(1)
Cu(1)–O(10)	1.980(3)	Cu(1)–O(11)	2.240(2)
Cu(1)–N(1)	2.039(2)	Cu(1)–N(2)	2.010(2)

2.4. *Antibacterial testing*

The *in vitro* antibacterial activity of the complexes was evaluated against *S. aureus*, *Bacillus subtilis*, and *Escherichia coli* using the disk diffusion method [41]. Bacterial suspensions of *S. aureus*, *B. subtilis*, and *E. coli* were prepared to contain about 10^7, 10^8, and 10^9 colony-forming units (cfu) mL^{-1}, respectively; 20 mL of beef extract peptone medium was poured

Table 3. Hydrogen bonding geometry (Å and °) for **1–4**.

D–H···A	d(D–H)	d(H···A)	d(D···A)	∠(DHA)
1				
O(10)–H(1 W)···O(5)#1	0.83	2.08	2.855(3)	156.1
O(10)–H(2 W)···O(5)	0.83	2.03	2.815(3)	159.1
O(11)–H(3 W)···O(21)#2	0.84	1.85	2.661(3)	161.1
O(11)–H(4 W)···O(16)	0.83	2.00	2.818(3)	168.0
O(12)–H(5 W)···O(20)#3	0.83	1.86	2.679(3)	173.9
O(12)–H(6 W)···O(8)#4	0.83	1.85	2.675(3)	170.3
O(13)–H(7 W)···O(9)#4	0.83	1.89	2.716(3)	174.4
O(13)–H(8 W)···O(9)	0.83	2.07	2.861(3)	159.0
O(14)–H(9 W)···O(17)#5	0.83	2.02	2.829(3)	167.7
O(14)–H(10 W)···O(18)#6	0.83	1.98	2.800(3)	168.5
O(15)–H(11 W)···O(6)#6	0.83	1.92	2.711(3)	158.7
O(15)–H(12 W)···O(4)#7	0.83	1.84	2.671(3)	174.6
O(16)–H(13 W)···O(18)#4	0.82	2.06	2.870(3)	166.9
O(16)–H(14 W)···O(8)#3	0.83	1.99	2.808(3)	169.2
O(17)–H(15 W)···O(19)#8	0.83	2.03	2.843(3)	167.8
O(17)–H(16 W)···O(5)#9	0.83	2.11	2.927(3)	170.6
O(18)–H(17 W)···O(20)	0.84	1.95	2.784(3)	173.7
O(18)–H(18 W)···O(9)	0.84	1.98	2.794(3)	163.8
O(19)–H(19 W)···O(1)#10	0.83	2.18	2.985(3)	164.1
O(19)–H(20 W)···O(7)	0.82	1.98	2.797(3)	169.1
O(20)–H(21 W)···O(19)	0.83	2.04	2.847(3)	164.5
O(20)–H(22 W)···O(4)#7	0.83	1.87	2.690(3)	173.3
O(21)–H(23 W)···O(16)#4	0.83	2.01	2.827(3)	166.3
O(21)–H(24 W)···O(17)#4	0.83	2.10	2.916(3)	168.8
Symmetry operations: #1 $-x$, $-y$, $-z$; #2 $x-1$, $y-1$, z; #3 x, $y-1$, z; #4 $-x+1$, $-y+1$, $-z+1$; #5 x, y, $z-1$; #6 $-x+1$, $-y+1$, $-z$; #7 $x+1$, $y+1$, z; #8 $-x$, $-y+1$, $-z+1$; #9 $-x$, $-y$, $-z+1$; #10 $-x$, $-y+1$, $-z$.				
2				
O(10)–H(1 W)···O(5)#1	0.82	1.80	2.612(2)	169.3
O(10)–H(2 W)···O(5)	0.83	2.18	2.925(2)	148.0
O(10)–H(2 W)···O(1)	0.83	2.25	2.952(2)	141.5
O(11)–H(3 W)···O(8)	0.83	2.04	2.843(2)	162.2
O(11)–H(4 W)···O(8)#2	0.82	1.94	2.706(2)	154.9
O(13)–H(8 W)···O(14)#3	0.82	2.02	2.746(3)	147.5
O(14)–H(9 W)···O(17)#3	0.84	2.00	2.819(4)	165.6
Symmetry operations: #1 $-x$, $-y+1$, $-z+1$; #2 $-x$, $-y$, $-z$; #3 $-x+1$, $-y+1$, $-z+1$.				
3				
O(5)–H(5)···O(9)#1	0.82	1.83	2.597(3)	154.8
O(10)–H(1 W)···O(8)#2	0.85	1.83	2.671(3)	172.8
O(10)–H(2 W)···O(8)	0.85	2.13	2.874(3)	146.1
O(11)–H(4 W)···O(9)#2	0.85	1.93	2.764(3)	166.4
O(11)–H(3 W)···O(6)#3	0.85	1.97	2.781(3)	160.5
C(4)–H(4)···O(6)#4	0.93	2.37	3.276(4)	165.3
C(21)–H(21A)···π#5	0.97	2.91	3.778(2)	149.7
Symmetry operations: #1 x, $y+1$, z; #2 $-x+1$, $-y+1$, $-z+1$; #3 $-x+1$, $-y+2$, $-z+1$; #4 $x+1$, y, z; #5 $-x+1$, $-y+1$, $-z+2$.				
4				
O(8)–H(8)···O(4)#1	0.82	1.75	2.539(2)	160.9
O(12)–H(5 W)···O(7)#2	0.84	2.08	2.860(2)	154.9
O(12)–H(6 W)···O(9)#3	0.83	2.08	2.892(3)	162.9
O(10)–H(1 W)···O(5)	0.82	1.98	2.739(2)	155.0
O(10)–H(2 W)···O(5)#4	0.82	1.96	2.722(2)	154.7
O(11)–H(3 W)···O(4)#4	0.83	1.92	2.738(2)	179.0
O(11)–H(4 W)···O(7)#5	0.83	2.02	2.814(2)	165.0
C(19)–H(19A)···π#6	0.97	2.78	3.675(2)	147.0
Symmetry operations: #1 x, y, $z-1$; #2 $x-1$, y, $z+1$; #3 x, y, $z+1$; #4 $-x+2$, $-y+1$, $-z+1$; #5 $-x+2$, $-y+1$, $-z$; #6 $-x+2$, $-y$, $-z+1$.				

into 100 mm × 15 mm sterile Petri dishes, and then 0.1 mL of the bacterial suspension was uniformly coated onto the beef extract peptone medium. The test solutions were prepared by measuring 10 mg of all selected substances which were dissolved in 10 mL of DMSO. Test solutions were added to 8-mm diameter filter paper disks and dried. The disks with tested substances and the blank (solvent) were added onto Petri dishes inoculated with the tested bacterial strains. After 24 h cultivation at 37 °C, diameters of zones of inhibition were determined; DMSO was inactive under applied conditions. The commercially available standard drug ampicillin was used as a reference.

3. Results and discussion

3.1. *Description of the structures*

3.1.1. Crystal structure of $\{[Co_{1.5}(L)(H_2O)_6]\cdot 6H_2O\}_n$ (1). Single-crystal X-ray diffraction analysis reveals that the asymmetric unit of **1** consists of one-and-a-half Co(II) ions, one L^{3-} ligand, six coordinated and six uncoordinated water molecules. Co1 is coordinated to two carboxylate oxygens from two L^{3-} ligands and four water molecules, while Co2 is six coordinate with one carboxylate and one ether oxygen from one L^{3-} ligand and four water molecules, as shown in figure 1(a). In **1**, the H_3L ligands are completely deprotonated and display a single-coordination mode [see scheme 1(A)]; every L^{3-} links two Co(II) ions. Three Co(II) ions are joined by two L^{3-} anions through four carboxylate and two ether oxygens to form a trinuclear unit [figure 1(b)]. The trinuclear units are connected into chains through O10–H1 W···O5 and O15–H12 W···O4 hydrogen bonds between water molecules and carboxylate oxygens, as shown in figure 1(c), which are further interlinked to a layer structure through O12–H6 W···O8 and O13–H7 W···O9 hydrogen bonds. Additionally, O11–H4 W···O16 and O16–H14 W···O8 hydrogen bonds between carboxylate oxygens and water molecules join the layers to a 3-D supramolecular structure, in which double-helical chains with left- and right-handed twists can be observed, the repeat unit can be described as –Co2–O12–H6 W···O8···H14 W–O16···H4 W–O11–Co2–O13–H7 W···O9–C12–C11–O3–C2–C1–O2–Co2–, and the pitch of the helix running along the *b*-axis is the same as the length of *b*-axis unit (10.13 Å), as shown in figure 1(d).

3.1.2. Crystal structure of $\{[Co_{1.5}(L)(4,4'\text{-bipy})_{1.5}(H_2O)_4]\cdot 4H_2O\}_n$ (2). There are one-and-a-half Co(II) ions, one L^{3-} ligand, one-and-a-half 4,4′-bipy ligands, four coordinated and four uncoordinated water molecules in the asymmetric unit of **2**. Co1 is six coordinate from two carboxylate oxygens from two L^{3-} ligands, two nitrogens from two 4,4′-bipy ligands, and two water molecules, while Co2 is six coordinate with two oxygens from one L^{3-} ligand, one nitrogen from 4,4′-bipy, and three waters, as shown in figure 2(a). Similar to **1**, in **2** H_3L ligands are completely deprotonated and show the same coordination mode as in **1** [see scheme 1(A)]. Each L^{3-} also links two Co(II) ions. Three Co(II) ions are joined by two L^{3-} ligands to form a trinuclear unit [figure 2(b)]. The 4,4′-bipy co-ligands display two coordination modes. One has a bridging coordination and the other is monodentate. Unlike **1**, those trinuclear units are bridged by 4,4′-bipy ligands to form a 1-D structure, as shown in figure 2(c). All the Co(II) ions of the chain are in a line. The chains are interlinked into a 2-D structure through O1O–H11 W···O5 and O11–H4 W···O8 hydrogen

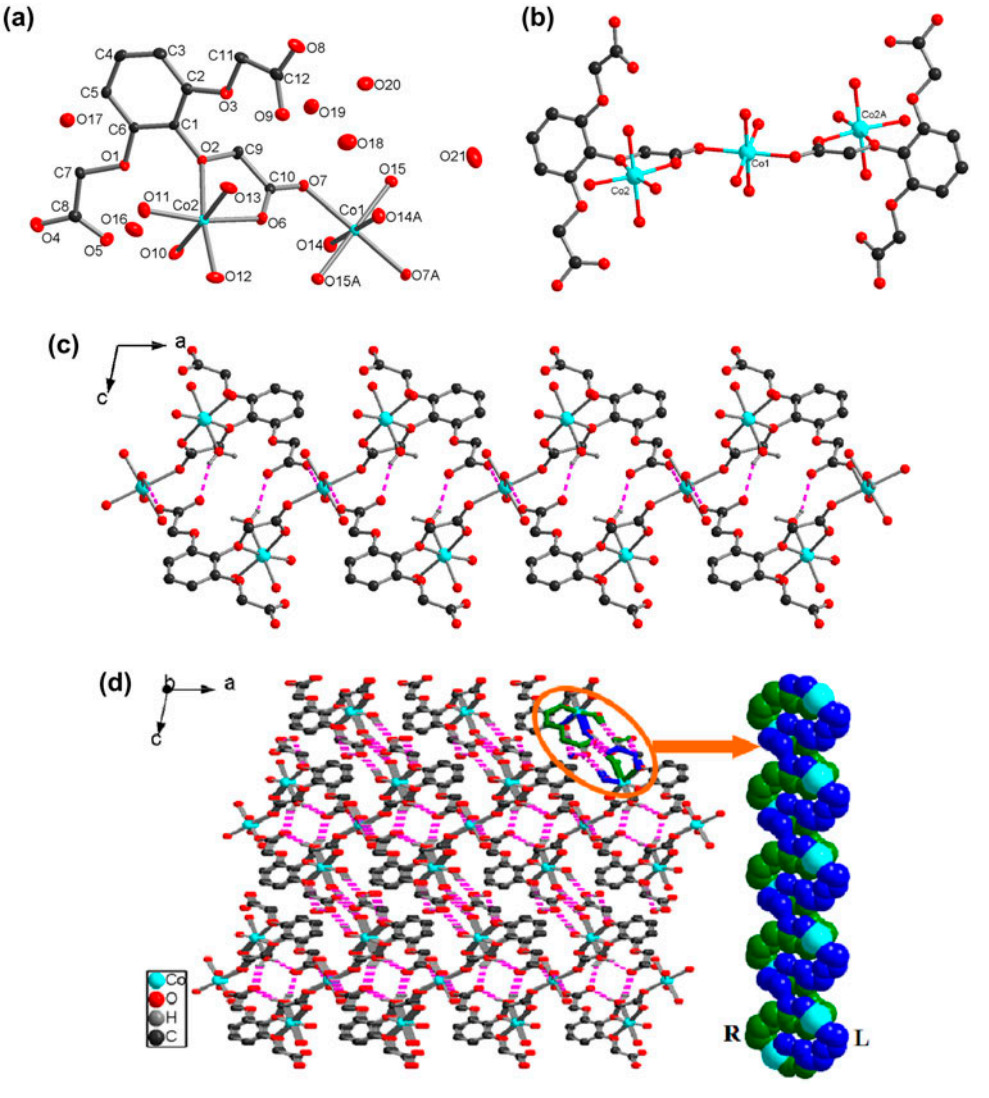

Figure 1. (a) Coordination environment of Co(II) in **1** with 30% thermal ellipsoids; all hydrogens are omitted for clarity. (b) Trinuclear unit in **1**. (c) 1-D structure of **1**. (d) 3-D supramolecular network of **1** along the *b*-axis with left-handed (blue) and right-handed (green) helices (see http://dx.doi.org/10.1080/00958972.2015.1082554 for color version).

bonds, which are further connected into a 3-D supramolecular network through O15–H12 W···O15 and C15–H15···O15 hydrogen bonds, in which meso-helical chains (left- and right-handed) can be observed. The repeat unit can be described as –Co1–O6–C20–O7–Co2–O10–H1 W···O5–C18–C17–O1–C16–C15–H15···O15– H12 W···O15–H15–C15–C16–O1–C17–C18···H1 W–O10–Co2–O7–C20–O6–, and the pitch of the helix running along the *b*-axis is the same as the length of *b*-axis unit (11.14 Å), as shown in figure 2(d).

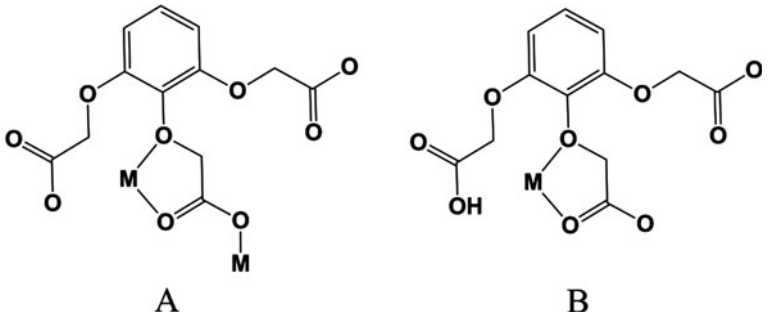

Scheme 1. The coordination modes of H_3L in **1** and **2** (M = Co) (A), **3** (M = Co), and **4** (M = Cu) (B).

3.1.3. Crystal structure of {[Co(HL)(2,2′-bipy)(H_2O)$_2$]·1.5H_2O}$_n$ (3). The asymmetric unit in **3** consists of one Co(II), one HL^{2-}, one 2,2′-bipy, two coordinated, and one and half uncoordinated water molecules. The Co(II) is coordinated to two oxygens from one HL^{2-}, two nitrogens from one 2,2′-bipy, and two oxygens from two waters [figure 3(a)]. In **3**, only two carboxylate groups of H_3L ligand are deprotonated and one deprotonated carboxylate is monodentate, while the other remains uncoordinated [see scheme 1(B)]. Each HL^{2-} chelates one Co(II) ion through one carboxylate oxygen and one ether oxygen of one acetate into a mononuclear unit, which is linked into a 1-D structure through O5–H5···O9 and O11–H1 W···O8 hydrogen bonds between water molecules and carboxylate oxygens, as shown in figure 3(b). The chains are further interlinked into a layer structure through O11–H4 W···O9 and C4–H4···O6 hydrogen bonds. Unlike **1** and **2**, in **3**, a 3-D supramolecular structure was formed by C–H···π interactions (as shown in table 3) between $-CH_2$ groups and the phenyl ring of adjacent HL^{2-} ligands, in which left- and right-handed helical chains can be observed, and the pitch of the helix running along the *b*-axis is the same as its length (11.30 Å) [figure 3(c)].

3.1.4. Crystal structure of {[Cu(HL)(phen)(H_2O)$_2$]·H_2O}$_n$ (4). Similar to **3**, in **4**, H_3L is partially deprotonated [see scheme 1(B)]. The asymmetric unit of **4** contains one Cu(II), one HL^{2-}, one phen, two coordinated, and one uncoordinated water molecules. The Cu(II) coordinates to one carboxylate oxygen and one ether oxygen of one oxyacetate, two nitrogens from one phen, and two waters, displaying a distorted octahedral geometry [figure 4(a)]. Complex **4** is also a 0-D structure, which is connected into a 1-D structure through O8–H8···O4, O10–H2 W···O5, and O11–H3 W···O4 hydrogen bonds between water molecules and carboxylate oxygen atoms, as shown in figure 4(b). The chains are further interlinked to a layer structure by O12–H5 W···O7 and O12–H6 W···O9 hydrogen bonds. Similar to **3**, a 3-D supramolecular network is formed by C–H···π interaction between $-CH_2$ groups and the phenyl rings of adjacent HL^{2-} ligands. Abundant intermolecular hydrogen bonds exist (as shown in table 3), in which double-stranded helical chains can be observed, and the pitch of the helix running along the *c*-axis is the same as the length of the *c*-axis unit (23.58 Å), as shown in figure 4(c).

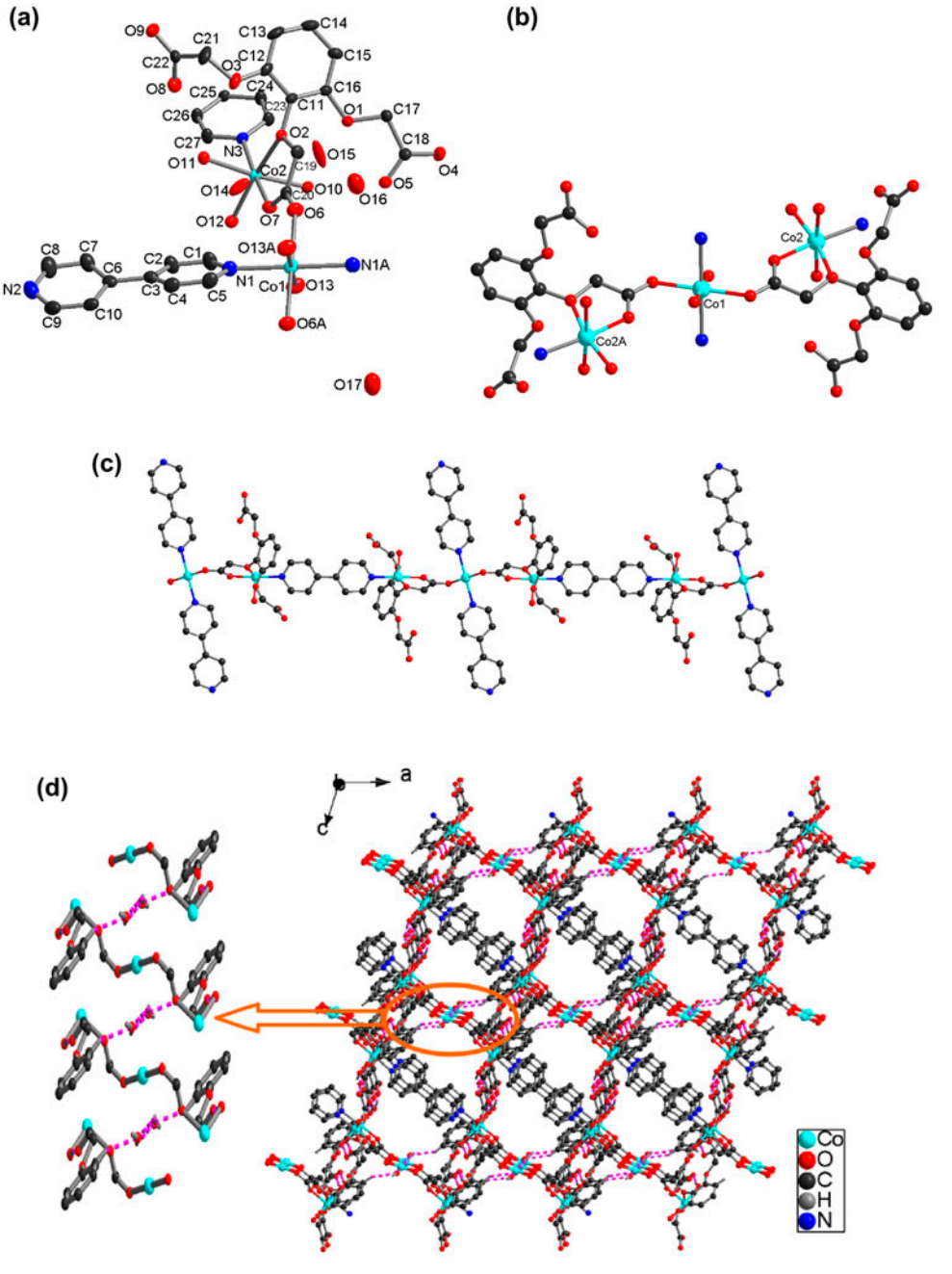

Figure 2. (a) Coordination environment of Co(II) in **2** with 30% thermal ellipsoids; all hydrogens are omitted for clarity. (b) Trinuclear unit in **2**. (c) 1-D chain structure of **2**; all water molecules and hydrogens are omitted for clarity. (d) The 3-D supramolecular network of **2** along the *b*-axis with meso-helical chains.

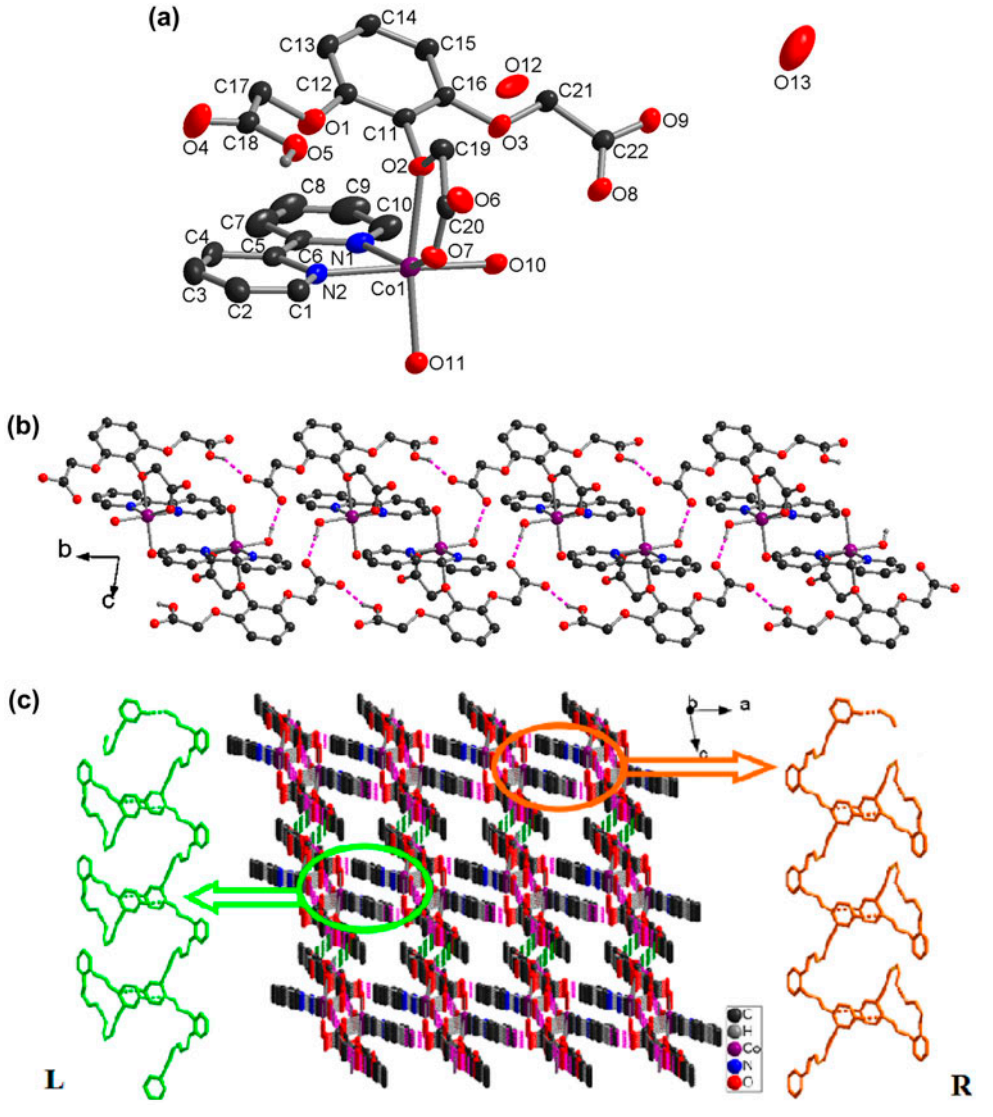

Figure 3. (a) Coordination environment of Co(II) in **3** with 30% thermal ellipsoids; all hydrogens except unprotonated carboxylate hydrogen are omitted for clarity. (b) 1-D chain structure of **3** along the *a*-axis. (c) 3-D supramolecular network of **3** along the *b*-axis with left-handed (bright green) and right-handed (orange) helices (see http://dx.doi.org/10.1080/00958972.2015.1082554 for color version).

3.2. *Comparison of the structures*

As shown in scheme 1, H_3L ligands exhibit two coordination modes. In **1** and **2**, H_3L ligands are completely deprotonated to L^{3-} and each L^{3-} connects two metal ions. However, in **3** and **4**, H_3L is partially deprotonated to generate HL^{2-} anions and each HL^{2-} anion bonds to only one metal ion. In **1–4**, Co(II)/Cu(II) ions are all six coordinate. In **1** and **2**, two L^{3-} ligands are connected by one Co1 and two Co2 ions to form a trinuclear

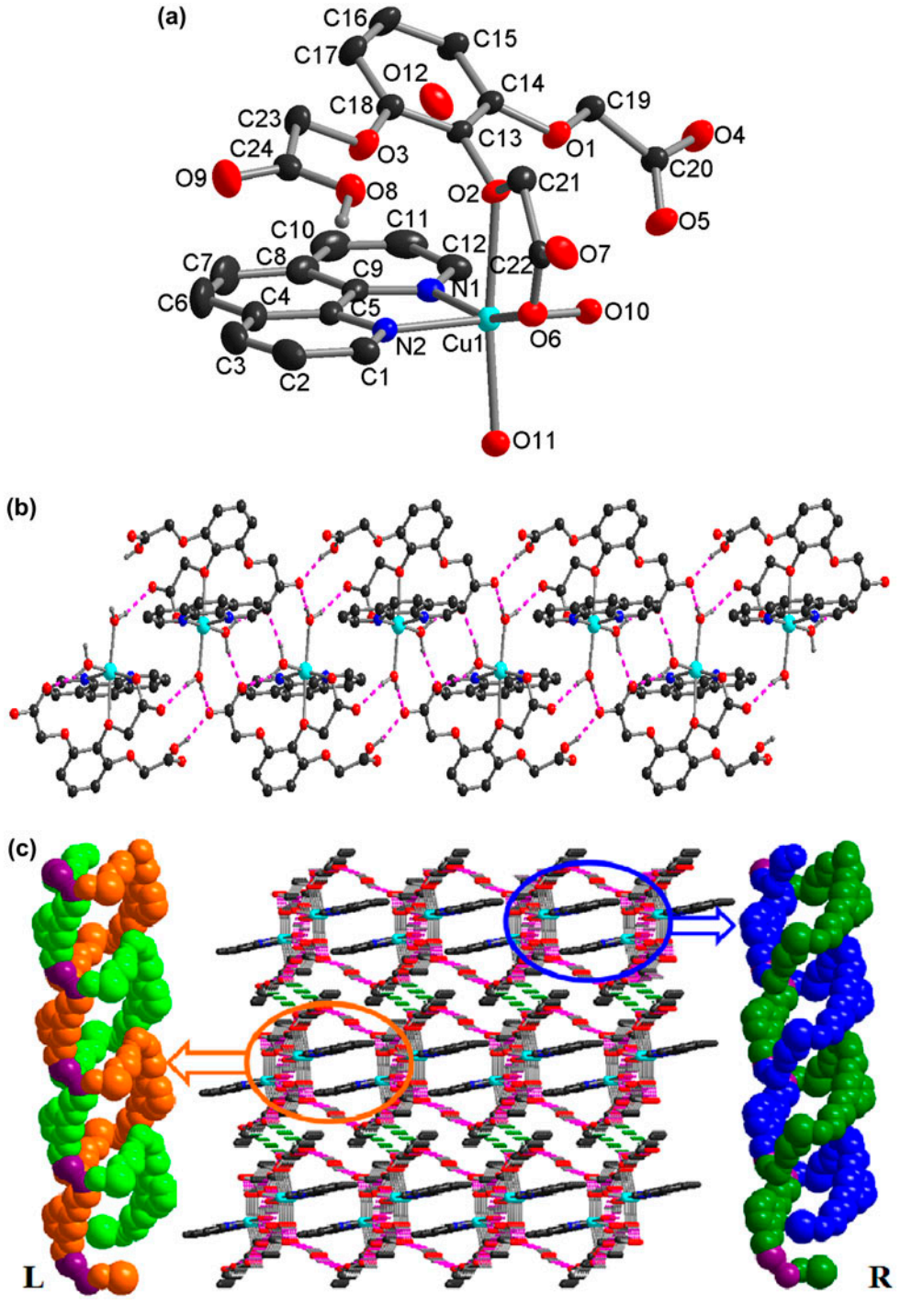

Figure 4. (a) Coordination environment of Cu(II) in **4** with 30% thermal ellipsoids; all hydrogens except unprotonated carboxylate hydrogen are omitted for clarity. (b) 1-D chain structure of **4** along the *a*-axis. (c) 3-D supramolecular network of **4** along the *c*-axis with double-stranded helices.

unit. In **2**, trinuclear units are interlinked by bridging 4,4′-bipy into a 1-D structure. Complexes **3** and **4** are mononuclear, in which Co(II)/Cu(II) ions have distorted octahedral geometry, coordinated by two water molecules, one carboxylate oxygen and one ether oxygen of one oxygen acetate group, and two nitrogens from chelating 2,2′-bipy or phen ligands. There is rich hydrogen bonding in **1–4**, such as O–H···O and C–H···π, which join the trinuclear units of **1**, the chains of **2**, and mononuclear units of **3** and **4** into 3-D supramolecular networks.

Cd/Zn/Co complexes based on benzene-1,2,3-triyltris(oxy)triacetic acid, $Cd_3L_2(H_2O)_3 \cdot H_2O$ (**5**), $Zn(HL)(phen)(H_2O)_2 \cdot H_2O$ (**6**), and $Co(HL)(phen)(H_2O)_2 \cdot H_2O$ (**7**), have been reported [42]. Compared with **1**, in **5**, H_3L is completely deprotonated to L^{3-} ions, and each L^{3-} joins five Cd ions to meet the need of larger radii and higher coordination number of Cd(II), further to form a 3-D metal–organic framework.

Complex **4** is isostructural to **6** and **7**. In **4**, **6**, and **7**, H_3L is partially deprotonated to HL^{2-} binding one metal(II) in mononuclear structures, which are further linked to 3-D supramolecular networks with O–H···O and C–H···π hydrogen bonding.

H_3L ligands join M(II) cations to double-stranded helical chains in **1** and **4**, meso-helices in **2**, and single-stranded helices in **3** with the aid of 2,2′-bipy. This is most likely due to H_3L ligand possessing a rigid benzene ring and three flexible O-acetate groups with a total of nine possible coordination sites. The functional groups also branch out with multiple angles of 60° and 120°, which help H_3L ligands to construct helical structures with metal ions.

3.3. *Antibacterial activity results*

The antibacterial activities of H_3L and **1–4** have been carried out against *S. aureus* and *B. subtilis* as Gram-positive bacteria and *E. coli* as Gram-negative bacteria. From the results given in table 4, no activity was observed against bacterial strains in pure DMSO. H_3L and **1–4** exhibit antibacterial activity against the tested bacteria. Complexes **1–4** and the corresponding metal salts have more activity against *S. aureus* than *B. subtilis* and *E. coli*, while they all exhibit weaker antibacterial activities than ampicillin. The activity of H_3L is enhanced against the tested bacteria after coordinating with metal ions. According to the literature, metal complexes usually have stronger antibacterial activities than the corresponding ligands. For example, 4-[phenyl(phenylimino)methyl]-benzene-1,3-diol and its Mn(II), Co(II), Ni(II), Cu(II), and Zn(II) complexes were synthesized and evaluated for their antibacterial activity, and the results of antibacterial test showed that the metal ion complexes displayed better antibacterial activities than the corresponding free ligands

Table 4. Zones of inhibition (diameter in mm) of H_3L and **1–4** against selected bacteria, including diameter of disk (8 mm).

Complexes	*S. aureus*	*B. subtilis*	*E. coli*
H_3L	11.2	9.1	+
1	15.4	10.8	11.0
2	14.7	11.5	10.8
3	15.3	11.4	10.4
4	15.5	10.6	10.5
$CoCl_2 \cdot 6H_2O$	10.2	8.8	9.7
$CuSO_4 \cdot 5H_2O$	10.6	9.0	10.3
Ampicillin	19.8	17.7	16.2
DMSO	–	–	–

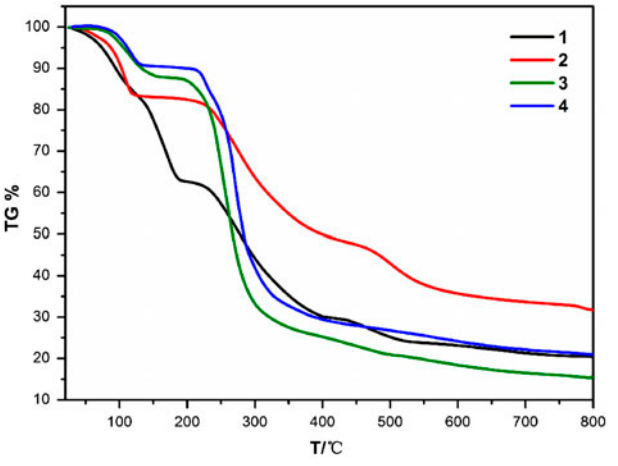

Figure 5. TGA curves of **1–4**.

against the tested bacteria [43]. Sang reported that a N,N′-bis(5-fluoro-2-hydroxybenzylidene)ethane-1,2-diamine-Mn(II) displayed good activity against *B. subtilis*, *S. aureus*, *E. coli*, and *P. fluorescens*, and exhibits stronger activity against the bacteria than its free Schiff base ligand [44]. The increase in antibacterial activity of complexes may be due to the chelation theory of Tweedy [45, 46].

3.4. *Thermogravimetric analyses (TGA)*

TGA of **1–4** were carried out to examine their thermal stabilities; TGA data were collected under N_2 with a heating rate of 10 °C/min from room temperature to 800 °C, as shown in figure 5. For **1**, the weight loss attributed to gradual release of six uncoordinated and six coordinated waters per unit cell is observed from 40 to 194 °C (obsd 36.21%, Calcd 35.89%), and the framework starts to decompose above 223 °C. Complex **2** expels four uncoordinated and four coordinated waters (obsd 18.73%, Calcd 18.85%) from 48 to 124 °C and then **2** shows no further weight loss below 230 °C. Complex **3** loses one-and-a-half uncoordinated and two coordinated waters (obsd 12.19%, Calcd 10.93%) from 65 to 146 °C and the dehydrated structure begin to decompose over 215 °C. Complex **4** loses 9.29% (Calcd 9.06%) weight from 80 to 148 °C that corresponds to one uncoordinated and two coordinated water molecules; **4** starts to decompose above 232 °C.

4. Conclusion

Four transition metal coordination polymers based on H_3L with both flexibility and rigidity, in the presence of N-donor ligands, have been presented. The study demonstrates that benzene-1,2,3-triyltris(oxy)triacetic acid is capable of rich coordination modes to metal centers and can form diverse helical chains. In addition, N-donor auxiliary ligands and extended hydrogen bonding interactions are important for the formation of the high-dimensional

supramolecular networks of **1–4**. Antibacterial activity screening shows that the complexes exhibit more activity than the free ligand against the tested bacteria.

Supplementary material

CCDC 1047290-1047293 contain the supplementary crystallographic data for **1–4**. These data can be obtained free of charge via http://www.ccdc.cam.ac.uk/conts/retrieving.html, or from the Cambridge Crystallographic Data Center, 12 Union Road, Cambridge CB2 1EZ, UK; Fax: (+44)1223–336-033; or E-mail: deposit@ccdc.cam.ac.uk.

Disclosure statement

No potential conflict of interest was reported by the authors.

Funding

This work was supported by the State Key Laboratory of Food Science and Technology of Nanchang University [grant number SKLF-ZZB-201519]; Bureau of Education of Jiangxi Province [grant number GJJ09064].

References

[1] C.Y. Gao, L. Zhao, M.X. Wang. *J. Am. Chem. Soc.*, **133**, 8448 (2011).
[2] P.A.N. Reddy, M. Nethaji, A.R. Chakravarty. *Inorg. Chem. Commun.*, **6**, 698 (2003).
[3] D.L. Reger, A. Debreczeni, A.E. Pascui, M.D. Smith. *Polyhedron*, **52**, 1317 (2013).
[4] G.P. Yang, Y.Y. Wang, H. Wang, C.J. Wang, G.L. Wen, Q.Z. Shi, S.M. Peng. *J. Mol. Struct.*, **888**, 366 (2008).
[5] Q.G. Zhai, X.Y. Wu, S.M. Chen, C.Z. Lu, W.B. Yang. *Cryst. Growth Des.*, **6**, 2126 (2006).
[6] A. Majumder, G. Pilet, M.T.G. Rodriguez, S. Mitra. *Polyhedron*, **25**, 2550 (2006).
[7] X. Zhang, Y.Y. Huang, Q.P. Lin, J. Zhang, Y.G. Yao. *Dalton Trans.*, **42**, 2294 (2013).
[8] D.C. Zhong, X.L. Feng, T.B. Lu. *CrystEngComm*, **13**, 2201 (2011).
[9] Y.Z. Zheng, Y.B. Zhang, M.L. Tong, W. Xue, X.M. Chen. *Dalton Trans.*, **38**, 1396 (2009).
[10] H. Wang, J. Yang, T.C.W. Mak. *New J. Chem.*, **38**, 4690 (2014).
[11] X. Li, R. Cao, Y.Q. Sun, Q. Shi, D.Q. Yuan, D.F. Sun, W.H. Bi, M.C. Hong. *Cryst. Growth Des.*, **4**, 255 (2004).
[12] H.L. Jiang, B. Liu, Q. Xu. *Cryst. Growth Des.*, **10**, 806 (2010).
[13] P.C. Cheng, P.T. Kuo, Y.H. Liao, M.Y. Xie, W. Hsu, J.D. Chen. *Cryst. Growth Des.*, **13**, 623 (2013).
[14] L. Han, M.C. Hong. *Inorg. Chem. Commun.*, **8**, 406 (2005).
[15] C.B. Liu, M.X. Yu, X.J. Zheng, L.P. Jin, S. Gao, S.Z. Lu. *Inorg. Chim. Acta*, **358**, 2687 (2005).
[16] Y.N. Gong, C.B. Liu, H.L. Wen, L.S. Yan, Z.Q. Xiong, L. Ding. *New J. Chem.*, **35**, 865 (2011).
[17] C.B. Liu, Y.N. Gong, Y. Chen, H.L. Wen. *Inorg. Chim. Acta*, **383**, 277 (2012).
[18] M. Monfort, I. Resino, M.S.E. Fallah, J. Ribas, X. Solans, M. Font-Bardia, H. Stoeckli-Evans. *Chem. Eur. J.*, **7**, 280 (2001).
[19] S.W. Hung, F.A. Yang, J.H. Chen, S.S. Wang, J.Y. Tung. *Inorg. Chem.*, **47**, 7202 (2008).
[20] H.L. Jiang, D. Feng, T.F. Liu, J.R. Li, H.C. Zhou. *J. Am. Chem. Soc.*, **134**, 14690 (2012).
[21] H. Liu, Y.L. Zou, L. Zhang, J.X. Liu, C.Y. Song, D.F. Chai, G.G. Gao, Y.F. Qiu. *J. Coord. Chem.*, **67**, 2257 (2014).
[22] K.K. Bania, G.V. Karunakar, K. Goutham, R.C. Deka. *Inorg. Chem.*, **52**, 8017 (2013).
[23] X.L. Zhao, X.Y. Wang, S.N. Wang, J.M. Dou, P.P. Cui, Z. Chen, D. Sun, X.P. Wang, D.F. Sun. *Cryst. Growth Des.*, **12**, 2736 (2012).
[24] K.L. Huang, X. Liu, J.K. Li, Y.W. Ding, X. Chen, M.X. Zhang, X.B. Xu, X.J. Song. *Cryst. Growth Des.*, **10**, 1508 (2010).
[25] R. Ramnauth, S. Al-Juaid, M. Motevalli, B.C. Parkin, A.C. Sullivan. *Inorg. Chem.*, **43**, 4072 (2004).
[26] Y.N. Gong, M. Meng, D.C. Zhong, Y.L. Huang, L. Jiang, T.B. Lu. *Chem. Commun.*, **48**, 12002 (2012).

[27] P. Deria, J.E. Mondloch, E. Tylianakis, P. Ghosh, W. Bury, R.Q. Snurr, J.T. Hupp, O.K. Farha. *J. Am. Chem. Soc.*, **135**, 16801 (2013).
[28] Y.N. Gong, C.B. Liu, Y. Ding, Z.Q. Xiong, L.M. Xiong. *J. Coord. Chem.*, **63**, 1865 (2010).
[29] C.B. Liu, H.L. Wen, Y.N. Gong, X.M. Liu, S.S. Tan. *Z. Anorg. Allg. Chem.*, **637**, 122 (2011).
[30] Y. Chen, C.B. Liu, Y.N. Gong, J.M. Zhong, H.L. Wen. *Polyhedron*, **36**, 6 (2012).
[31] G.S. Yang, L. Li, C.B. Liu, H. Liu, Y.H. Wen, H.L. Wen. *Polyhedron*, **72**, 83 (2014).
[32] P. Pachfule, R. Das, P. Poddar, R. Banerjee. *Inorg. Chem.*, **50**, 3855 (2011).
[33] P.F. Shi, Z. Chen, G. Xiong, B. Shen, J.Z. Sun, P. Cheng, B. Zhao. *Cryst. Growth Des.*, **12**, 5203 (2012).
[34] B. Pan, R.Z. Huang, L.K. Zheng, C. Chen, S.Q. Han, D. Qu, M.L. Zhu, P. Wei. *Eur. J. Med. Chem.*, **46**, 819 (2011).
[35] D. Zhao, C. Chen, H.Y. Liu, L.K. Zheng, Y. Tong, D. Qu, S.Q. Han. *Eur. J. Med. Chem.*, **87**, 500 (2014).
[36] A. Mukherjee, G.R. Desiraju. *Chem. Commun.*, **47**, 4090 (2011).
[37] C.Y. Sun, E.B. Wang, D.R. Xiao, H.Y. An, L. Xu. *J. Mol. Struct.*, **741**, 149 (2005).
[38] Y. Zhang, J. Yang, Y. Yang, J. Guo, J.F. Ma. *Cryst. Growth Des.*, **12**, 4060 (2012).
[39] G.M. Sheldrick. *SADABS, Program for Empirical Absorption Correction of the Area Detector Data*, University of Göttingen, Germany (1997).
[40] G.M. Sheldrick. *Acta Crystallogr., Sect. A*, **64**, 112 (2008).
[41] A.W. Bauer, W.M.M. Kirby, J.C. Sherris, M. Turck. *Am. J. Clin. Pathol.*, **45**, 493 (1966).
[42] Y. Gong, P.G. Jiang, J. Li, T. Wu, J.H. Lin. *Cryst. Growth Des.*, **13**, 1059 (2013).
[43] P. Subbaraj, A. Ramu, N. Raman, J. Dharmaraja. *J. Coord. Chem.*, **67**, 2764 (2014).
[44] Y.L. Sang, X.C. Li, W.M. Xiao. *J. Coord. Chem.*, **66**, 4015 (2013).
[45] B.G. Tweedy. *Phytopathology*, **55**, 910 (1964).
[46] M. Tumer, D. Ekinci, F. Tumer, A. Bulut. *Spectrochim. Acta, Part A: Mol. Biomol. Spectrosc.*, **67**, 916 (2007).